Electronic Supplementary Material (ESI) for CrystEngComm.

Supporting Information

Tailoring adsorption induced switchability of a pillared layer MOF by crystal size engineering

Leila Abylgazina[a], Irena Senkovska*[a], Sebastian Ehrling[a], Volodymyr Bon[a], Petko St. Petkov[b], Jack D. Evans[a], Svetlana Krylova[c], Alexander Krylov[c], and Stefan Kaskel*[a]

Chair of Inorganic Chemistry I, Technische Universität Dresden, Bergstr. 66, 01069 Dresden, Germany

Content

1. Characteristic geometric parameters in $[M_2(bdc)_2dabco]_n$ and $[M_2(2,6\text{-}ndc)_2dabco]$ (DUT-8(M) (M: Ni, Co, Zn)

Table S1. Bond lengths and angles in DUT-8(M) (M = Ni, Co, Zn) (crystallographic data).

	M—O / Å	**M—N / Å**	**M…M / Å**	**M-M-N angle / °**
M = Ni				
$Ni_2(bdc)_2dabco$[1]	1.966(1)	2.053(1)	2.683(8)	180.0
DUT-8(Ni)_*op*[2]	1.983(7) - 2.008(7)	2.042(1)	2.653(5)	177.59(9)
DUT-8(Ni)_*cp*[2]	1.787(5) - 2.425(2)	1.905(8) 2.085(6)	2.735(9)	153.92(5)
M = Co				
$Co_2(bdc)_2dabco$[3]	2.028(2)	2.092(5)	2.683(5)	180.0
DUT-8(Co)_*op*[2]	2.027(3) - 2.031(3)	2.110(7)	2.691(2)	171.81(8)
DUT-8(Co)_*cp*[2]	1.70(9) - 2.20(7)	2.15(9) 2.13(9)	2.636(3)	141.50(0)
M = Zn				
$Zn_2(bdc)_2dabco$[4]	2.0314(2)	2.0440(4)	2.9521(9)	180.0
DUT-8(Zn)_*op*	2.029(4) 2.034(4)	2.076(7)	2.962(8)	178.26(15)
DUT-8(Zn)_*cp*	1.638(2) - 2.548(6)	2.293 2.098	3.804	112.02(3) 117.31(4)

2. PXRD patterns of as made samples in *N,N*-dimethylformamide

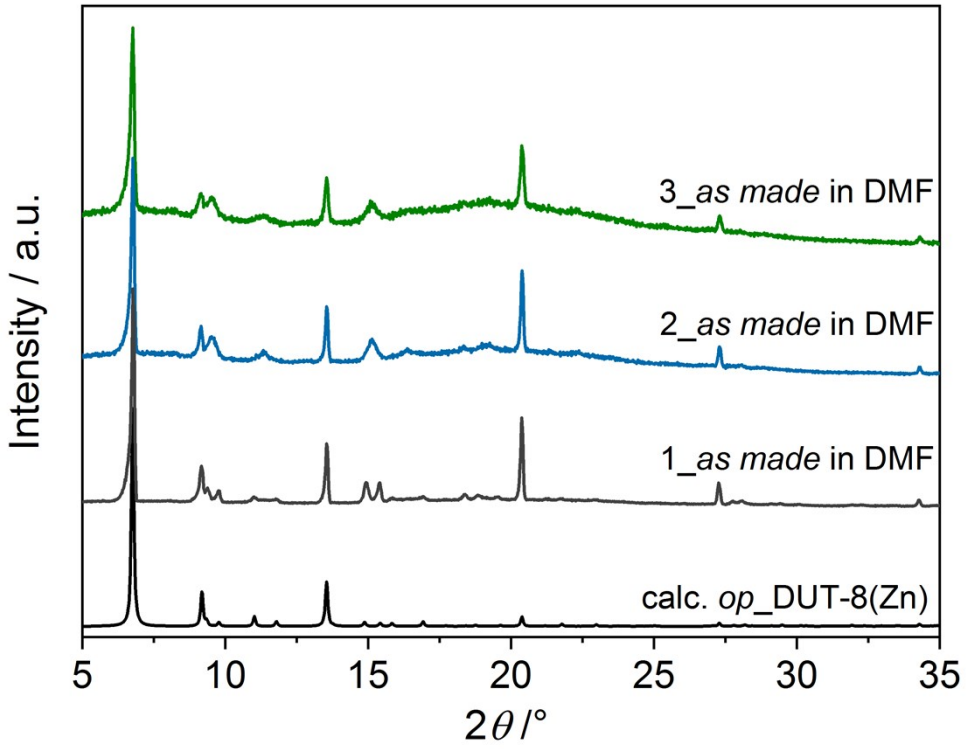

Figure S1. PXRD patterns of 1_macro-, 2_micron-, 3_submicron-sized particles of DUT-8(Zn) after synthesis in comparison with the pattern calculated from the single crystal structure.

3. Thermogravimetric analysis

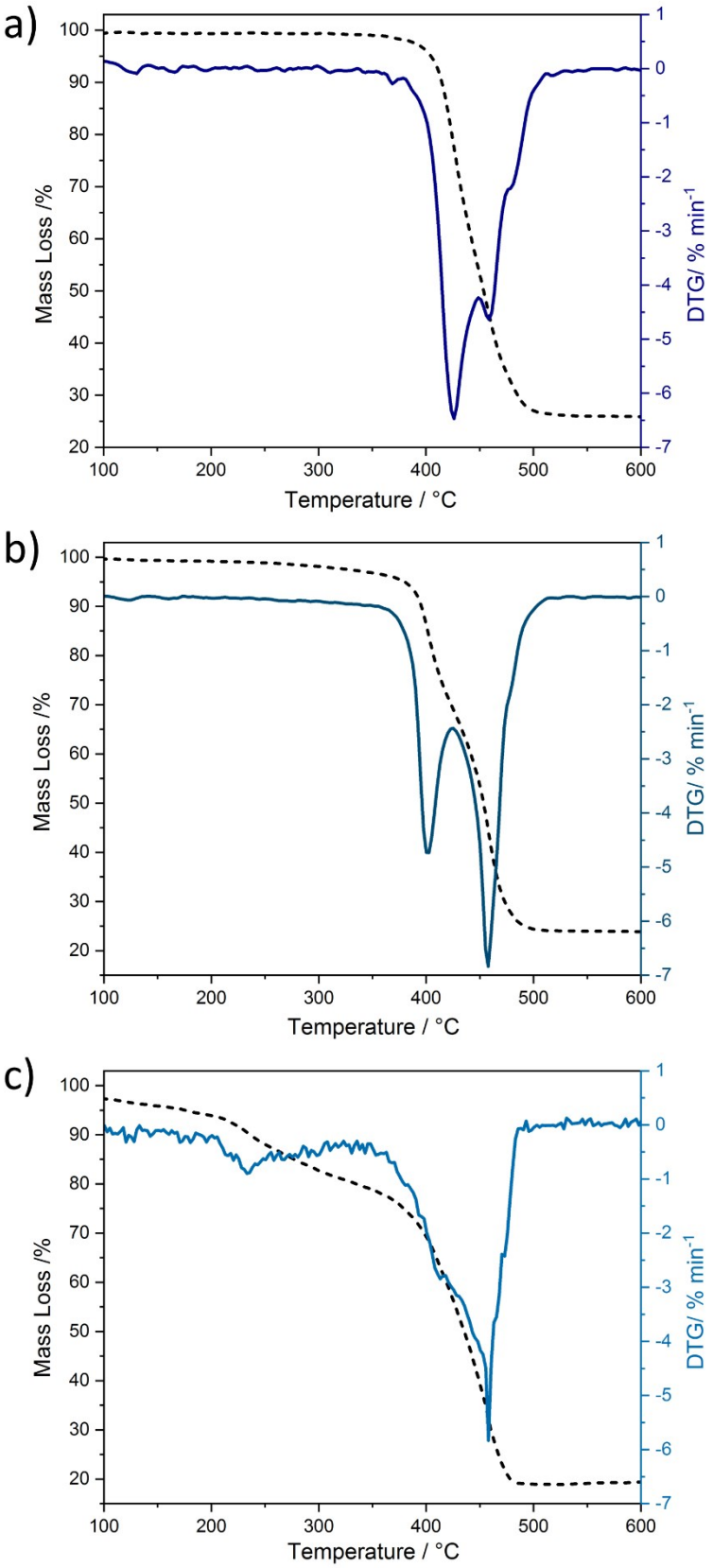

Figure S2. TGA (black) and DTG (blue) of: a) **1b** macro-sized sample; b) **2b** micron-sized sample; c) **3c** submicron-sized sample.

4. NMR spectroscopy

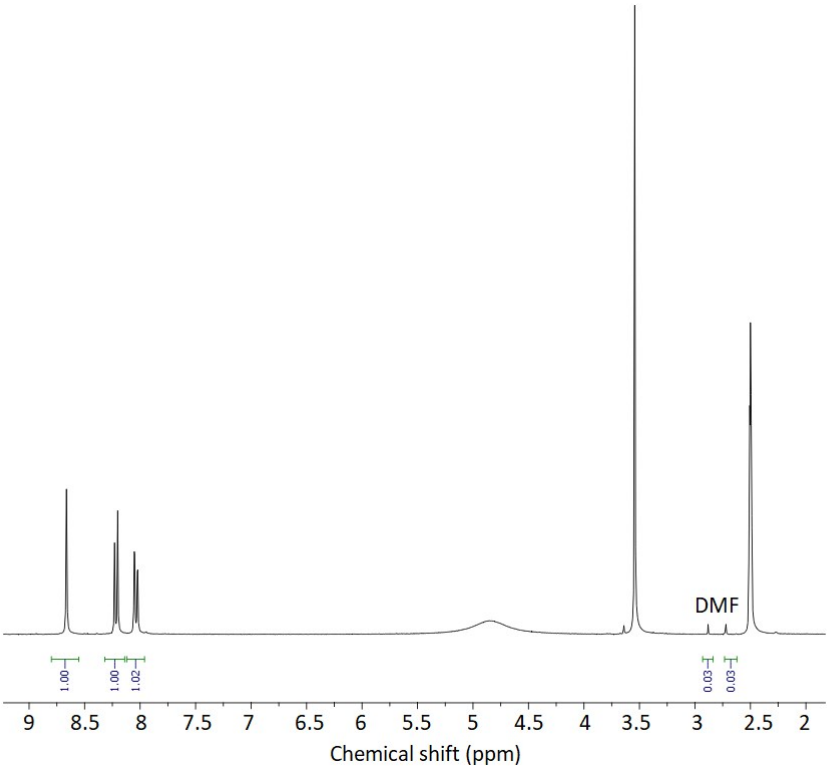

Figure S3. a) NMR spectra of **1a** macro-sized sample digested in DCl/D_2O d6-DMSO.

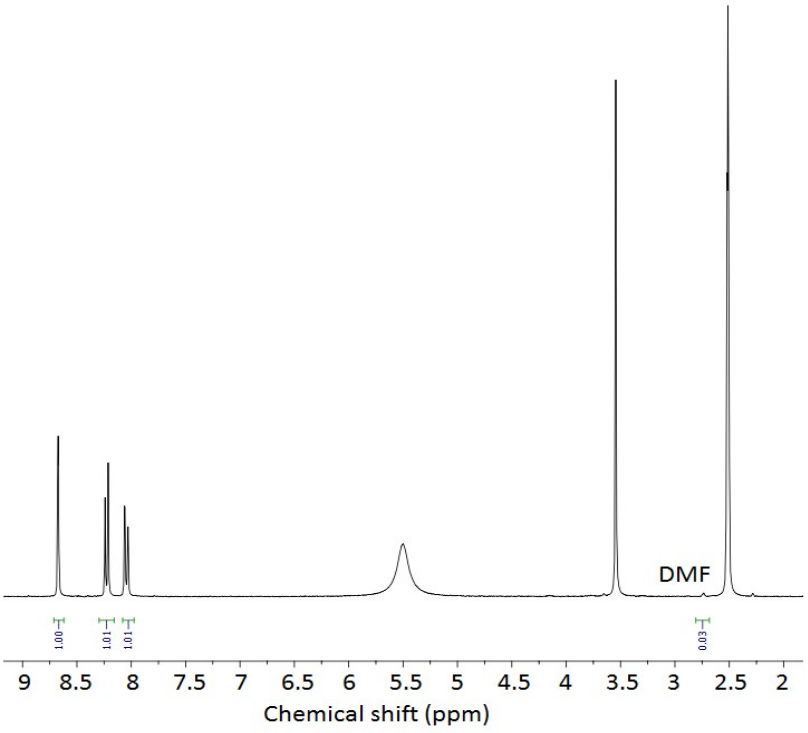

Figure S3. b) NMR spectra of 2**a** micron-sized sample digested in DCl/D_2O d6-DMSO.

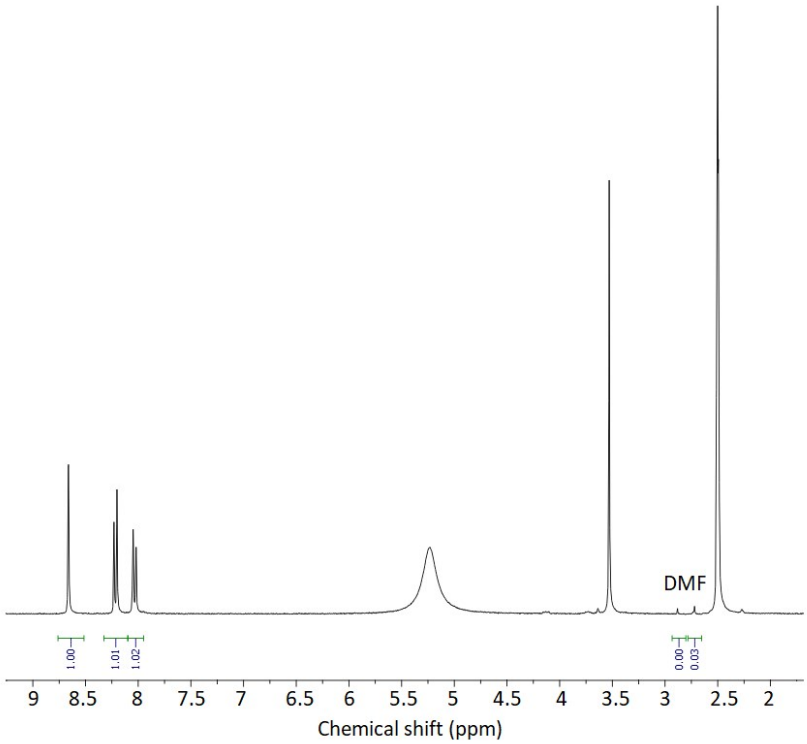

Figure S3. c) NMR spectra of 3**a sub**micron-sized sample digested in DCl/D_2O d6-DMSO.

5. Rietveld plot of the closed phase of DUT-8(Zn), **1b**_*cp*.

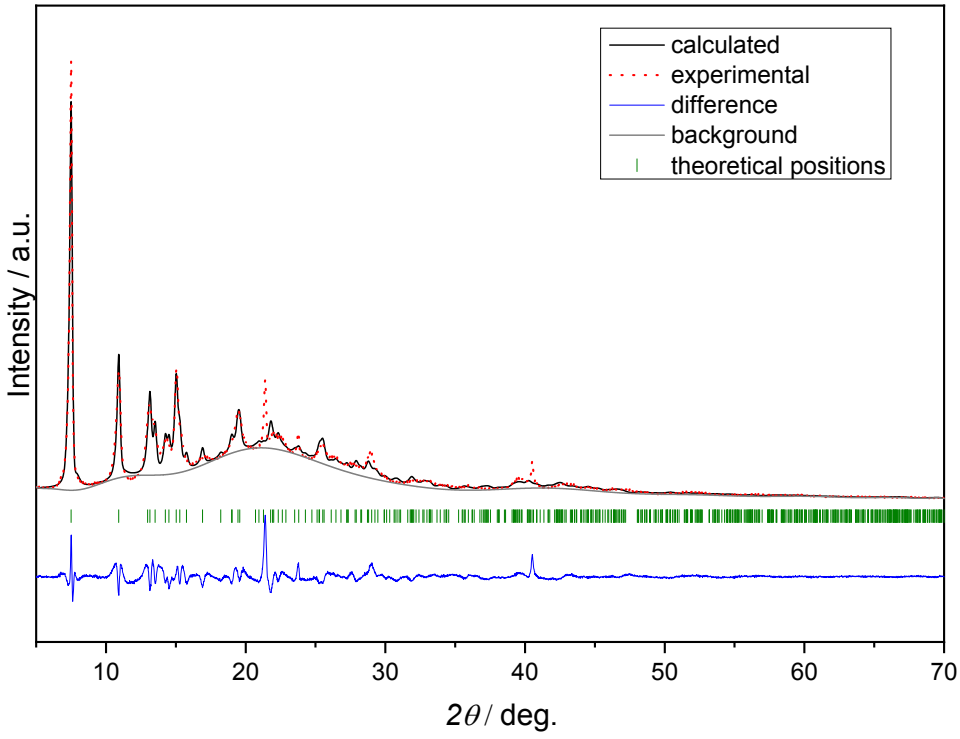

Figure S4. Rietveld plot of the closed pore phase of DUT-8(Zn), (**1b**_*cp*).

6. Additional PXRD patterns collected after adsorption measurements.

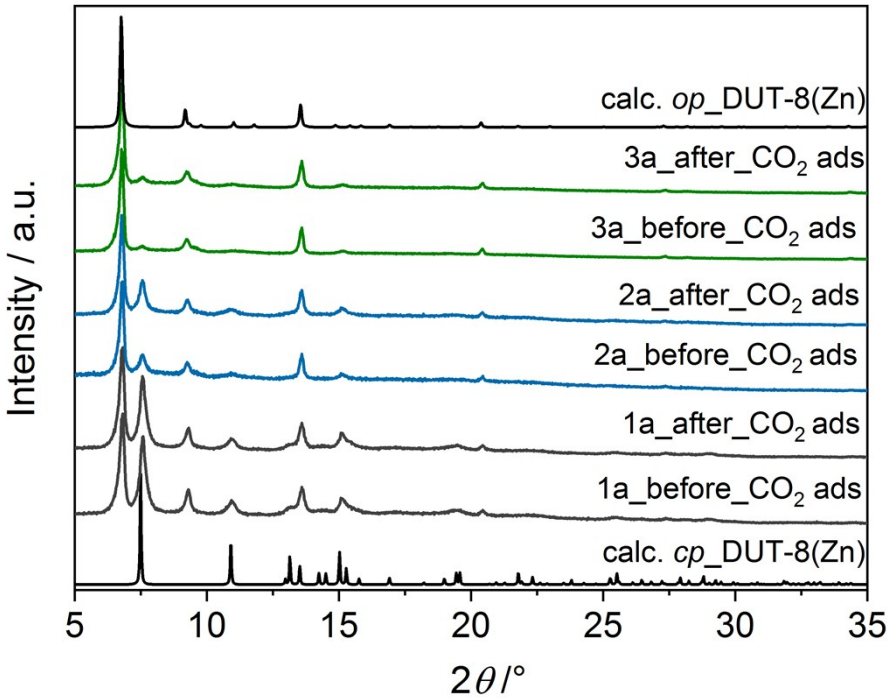

Figure S5. PXRD patterns of **1b** macro-, **2b** micron-, **3c** submicron-sized samples desolvated from DMF, before and after CO_2 physisorption measurements.

7. In situ PXRD during adsorption of chloromethane at 249 K.

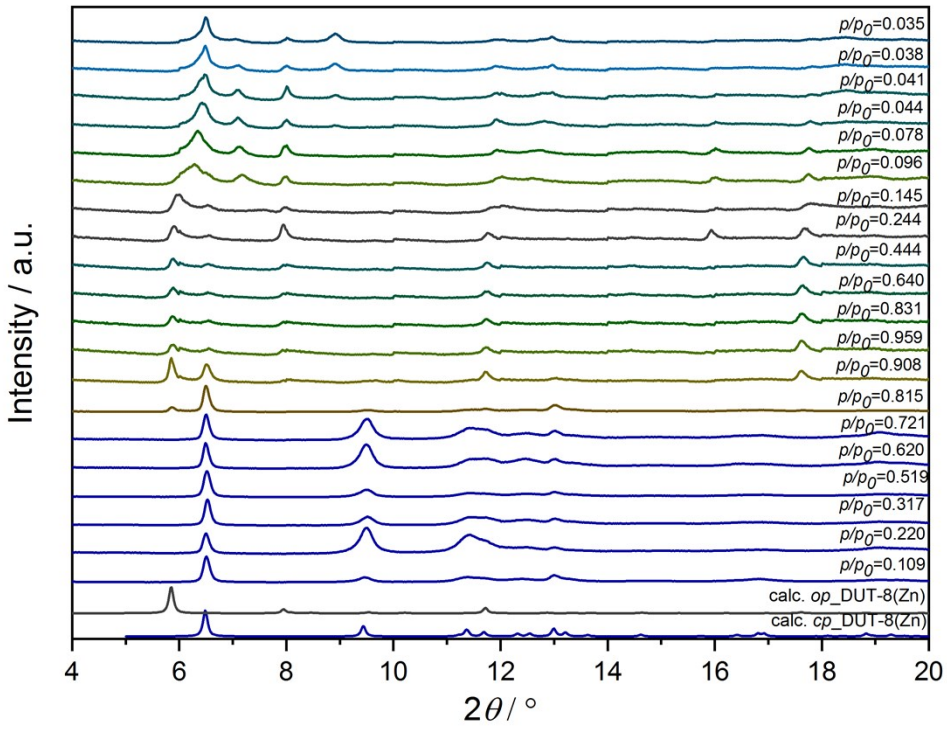

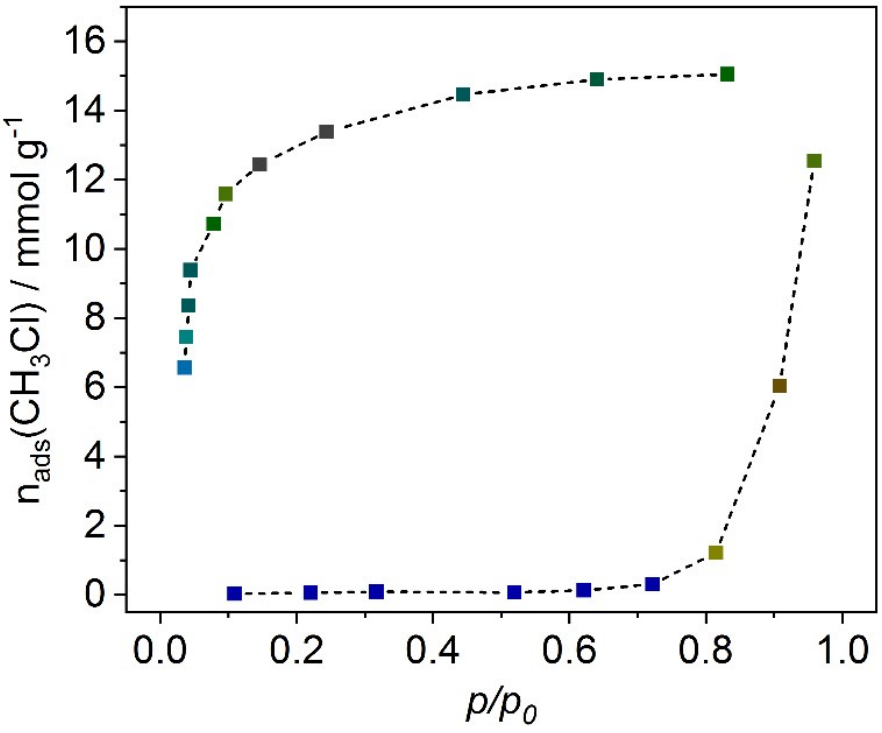

Figure S6. *In situ* PXRD patterns collected during CH_3Cl adsorption at 249 K on **1b** macro-sized sample (top) and corresponding isotherm (bottom)**.**

8. Additional vapor adsorption experiments.

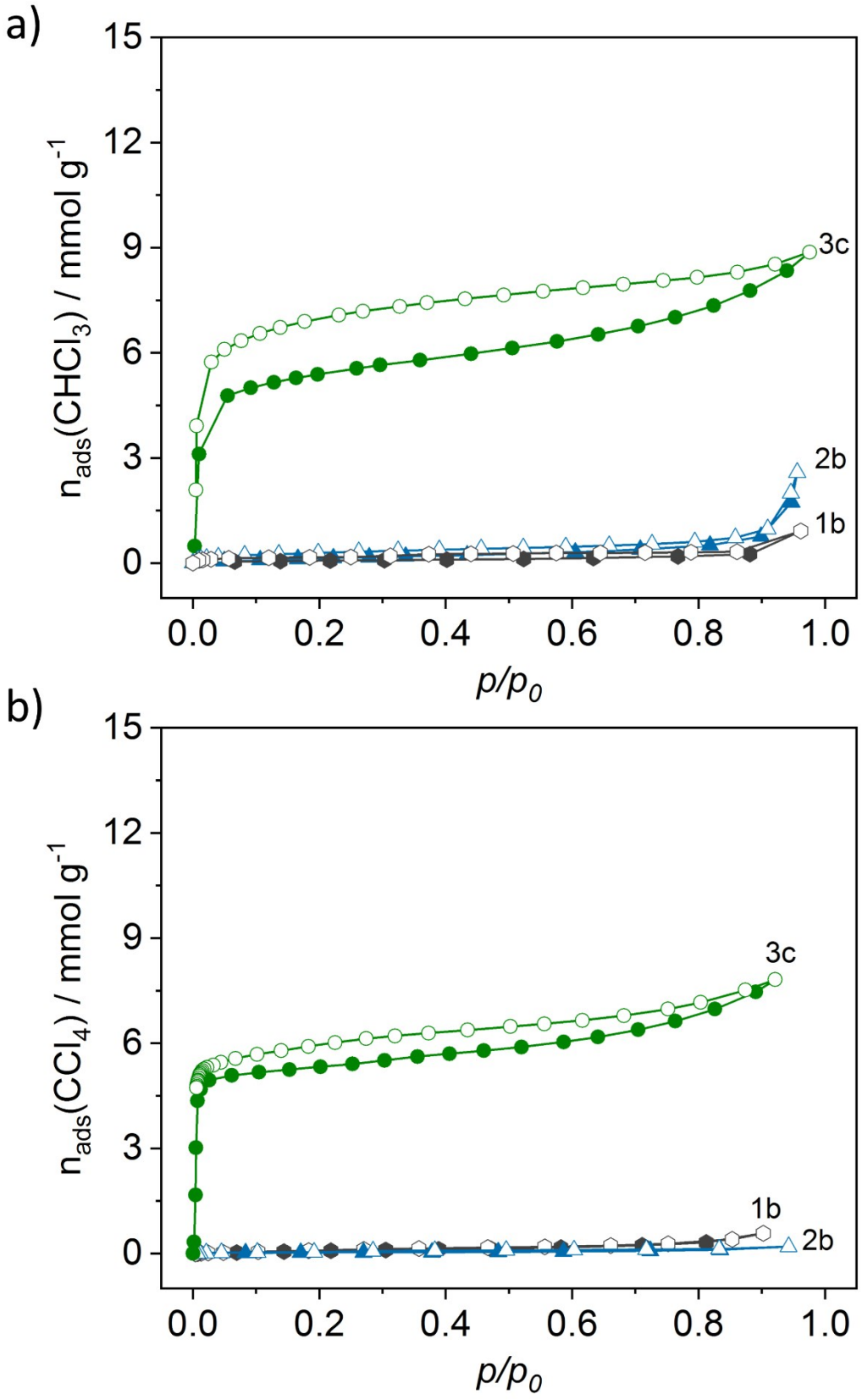

Figure S7. a) $CHCl_3$ and b) CCl_4 adsorption (filled symbols) and desorption (empty symbols) for **1b** macro-, **2b** micron-, **3c** submicron-sized samples of DUT-8(Zn).

9. *In situ* PXRD carbon dioxide adsorption at 195 K.

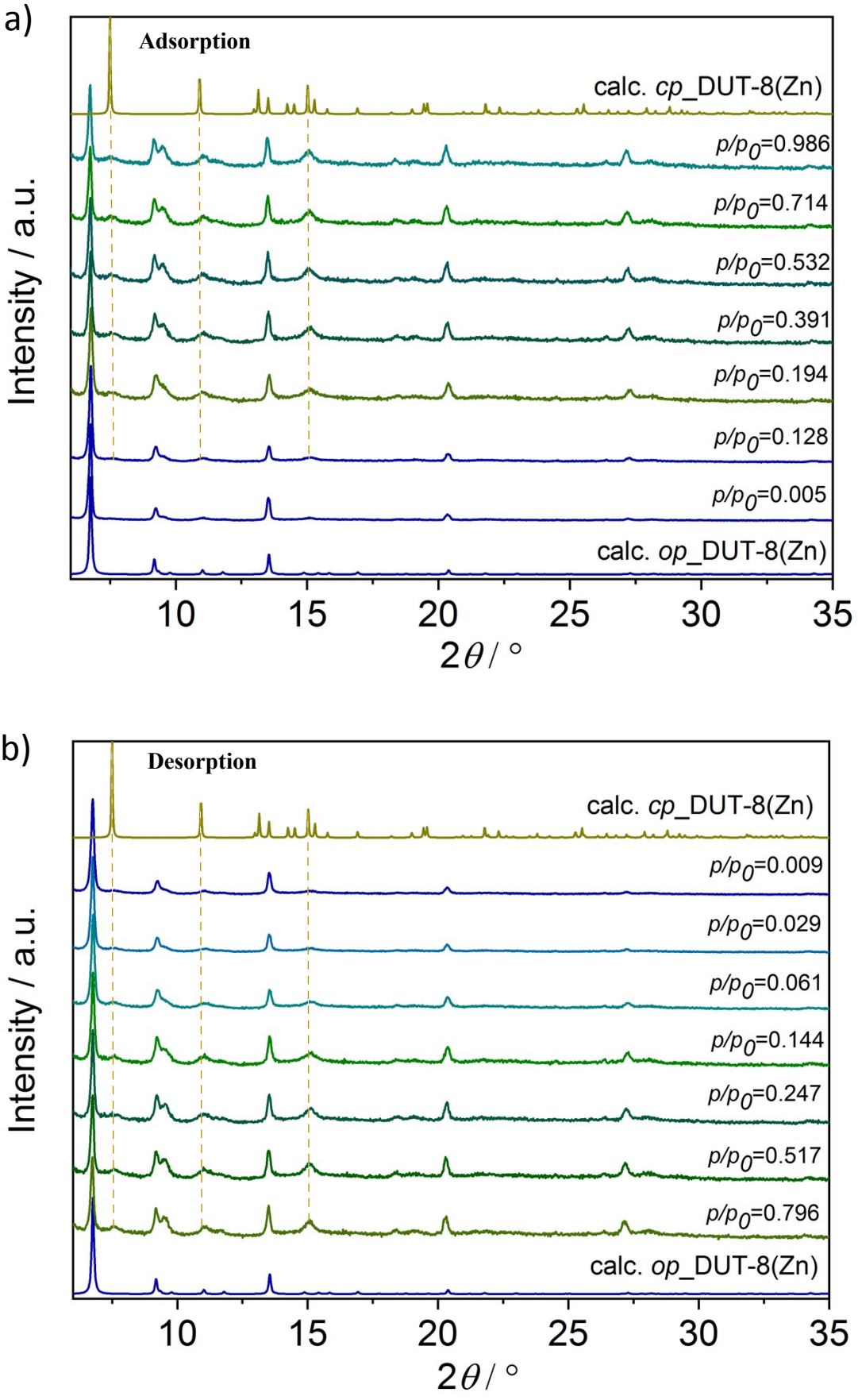

c)

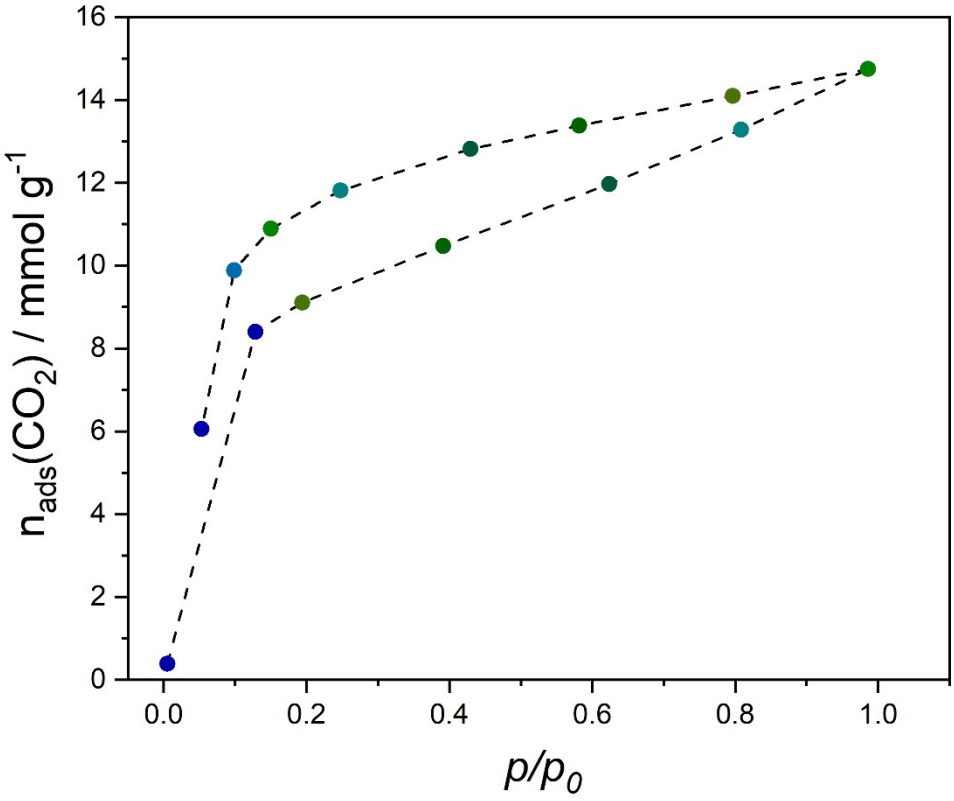

Figure S8. PXRD patterns collected during *in situ* CO_2 adsorption (a) and desorption (b) at 195 K on submicron-sized sample **3c**; c) corresponding in situ physisorption isotherm**.**

10. Raman spectroscopy.

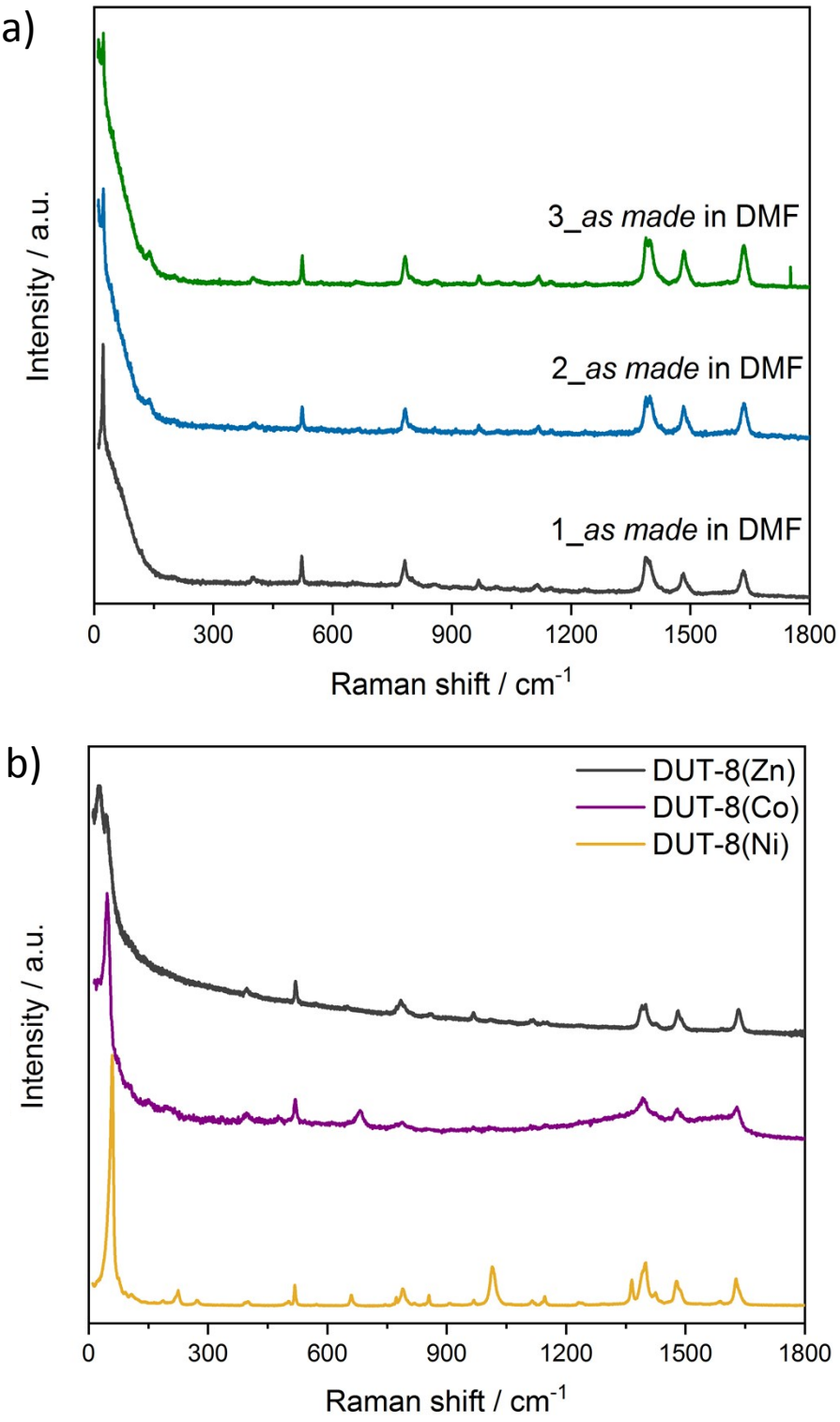

Figure S9. a) Full Raman spectra for samples solvated with DMF; b) Raman spectra of **1b**_*cp* DUT-8(Zn) in comparison with DUT-8(Ni) and DUT-8(Co)**.**

11. Dichloromethane adsorption isotherms

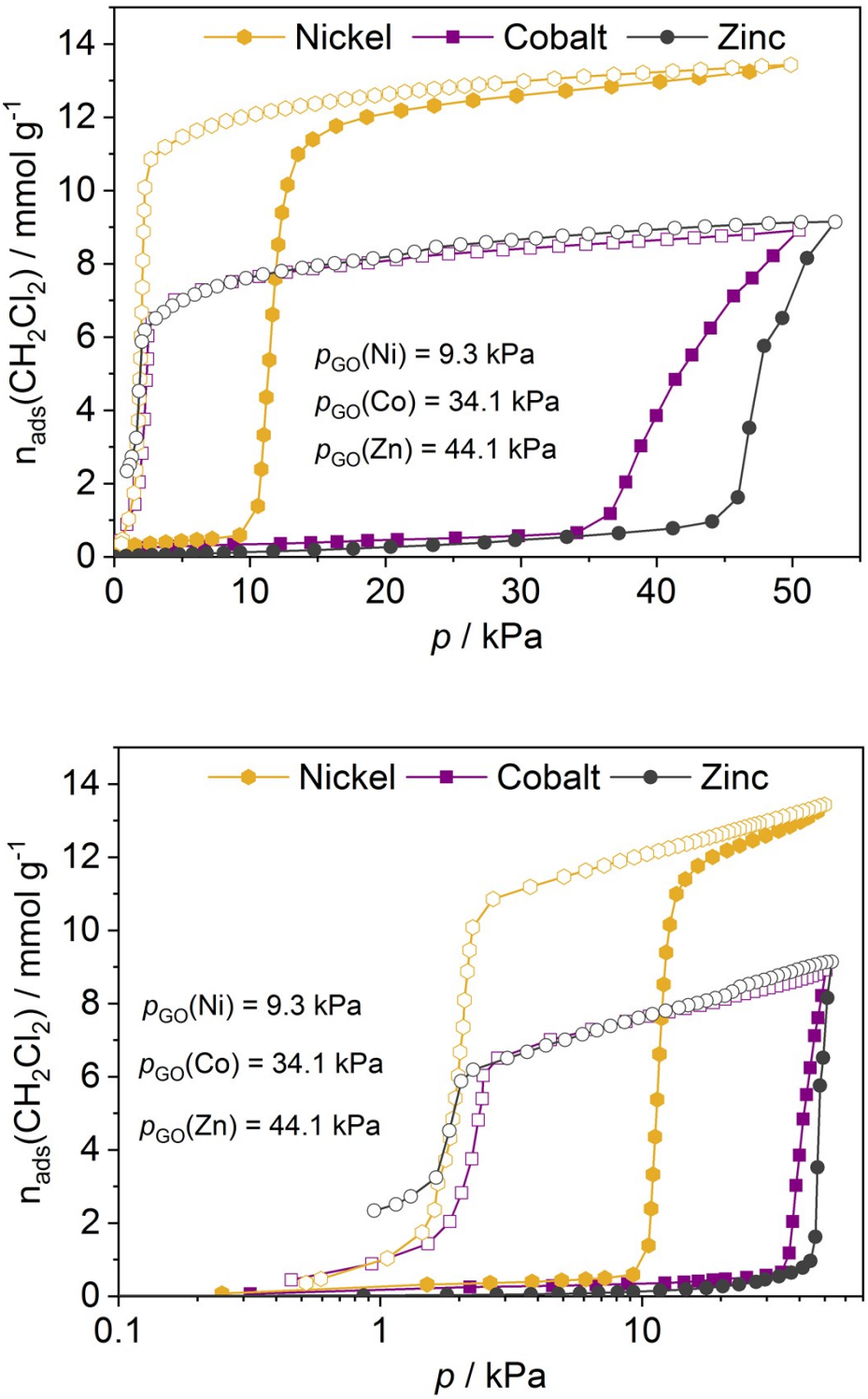

Figure S10. Dichloromethane adsorption isotherms (298 K) for macro-sized *cp* samples DUT-8(Ni), DUT-8(Co), DUT-8(Zn).

12. Infrared spectroscopy.

Table S2. Wavenumbers of expected and observed vibrations.

Vibration	***v*** **observed in 1b_*cp*** **/ cm^{-1}**	***v*** **observed in 2b_*cp*** **/ cm^{-1}**	***v*** **observed in 3c_*op*** **/ cm^{-1}**
$\boldsymbol{\nu_{as}(COO)}$	1602	1602	1605
$\boldsymbol{\nu_{s}(COO)}$	1467	1467	1465
$\boldsymbol{\delta_{oop}COO^-}$	806	806	813
$\boldsymbol{\nu_{as}NC_3}$	1056	1056	1056
$\boldsymbol{\nu_{s}NC_3}$	780	780	782

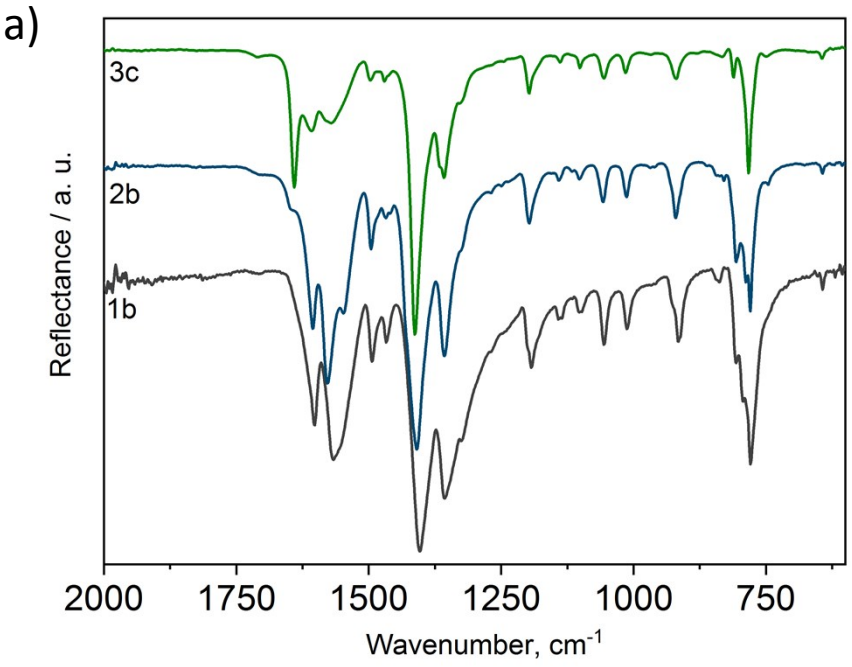

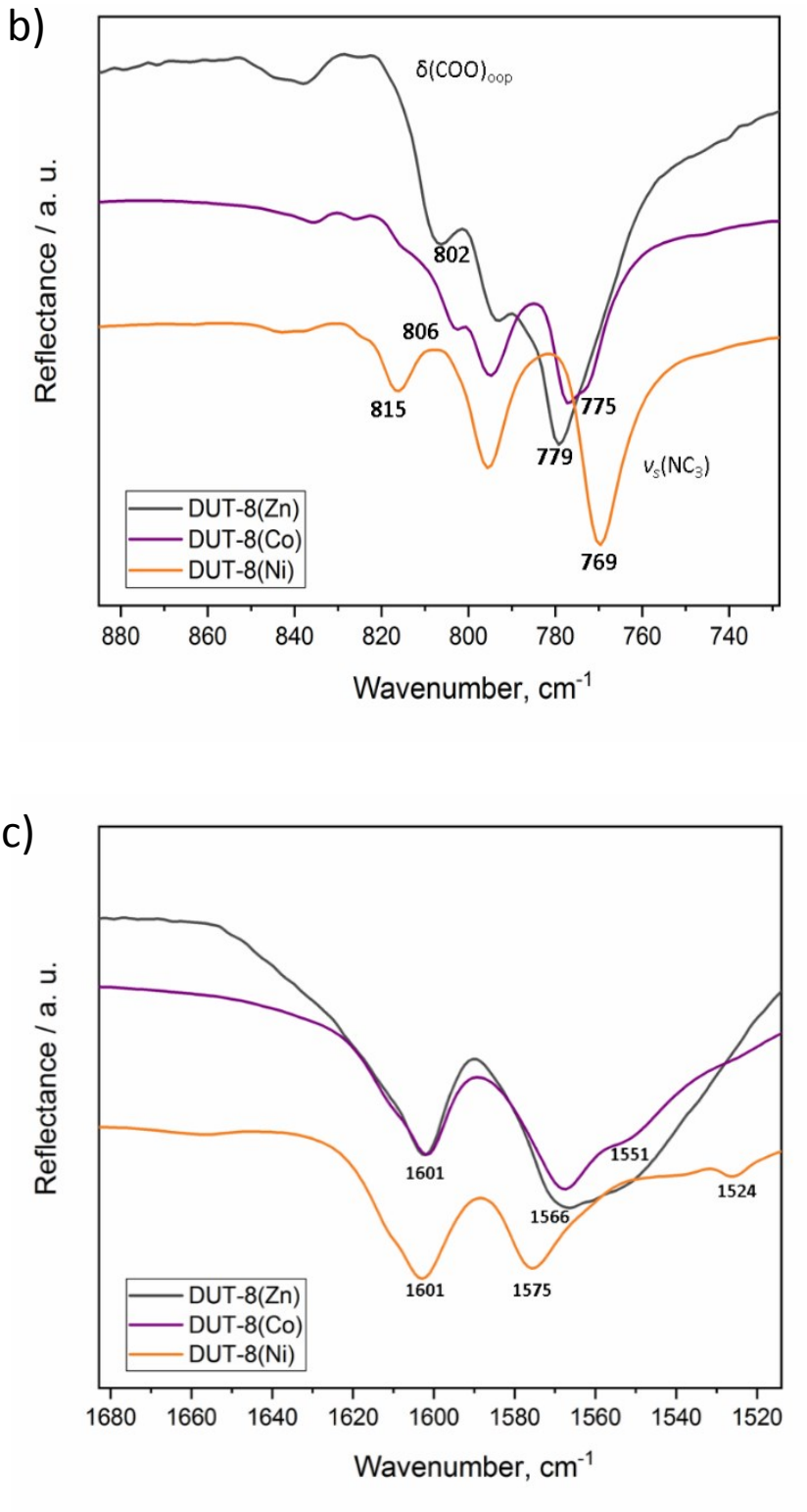

Figure S11. a) IR-spectra of **1b** macro-, **2b** micron-, **3c** submicron-sized samples DUT-8(Zn); b) and c) IR-spectra of DUT-8(Ni), DUT-8(Co), and DUT-8(Zn) in the closed pore state.

13. DFT results

Table S3. Relative energy for the constrained geometry scans of the M-M-N for the representative Zn paddle wheel.

Zn-Zn-N angle / °	**relative energy / kJ mol^{-1}**
180	0.00
175	0.04
170	0.54
165	1.61
160	3.36
155	5.92
150	9.53

Table S4. Characteristic geometric parameters in DUT-8(Zn): Zn…Zn distance in the paddle wheel, Zn-O(carboxylic) bond lengths, Zn-N(dabco) bond lengths, and Zn-Zn-N(dabco) angle.

Distances and angles	*op*	*cp*
Zn…Zn / Å	2.82	3.78
Zn – O / Å	2.06	1.99, 2.02, 2.02, 3.78
		2.03, 2.01, 2.11, 3.61
Zn – N / Å	2.10, 2.11	2.11, 2.14
Zn – Zn – N / °	174	119

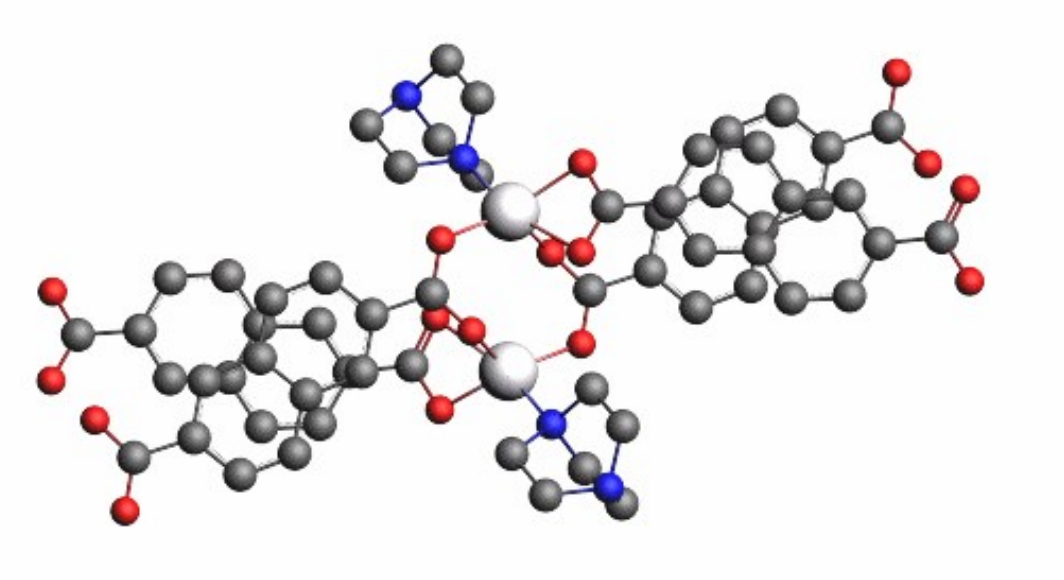

Figure S12. Geometry of distorted paddle wheel unit: cut from the periodic structure, in the calculated *cp* phase. Hydrogen atoms are omitted for clarity.

Table S5. Relative energy (ΔE) of the transformation of open to closed forms for DUT-8(Zn) and DUT-8(Ni),[5] change of strain energy E_{str} and change of London dispersion energy ΔE_{disp}. All values are in kJ mol^{-1} per formula unit.

	DUT-8(Zn)	DUT-8(Ni)
ΔE	-104	-86
E_{str}[a]	+78	+102
ΔE_{disp}[b]	-182	-188

[a] The strain energy E_{str} was calculated as follows: from total energy of each system the corresponding dispersion energy was removed. The resulting value for closed pore form was subtracted from the one of the open pore form.
[b] The change in the dispersion energy ΔE_{disp} was calculated as follows: the dispersion energy in the closed pore form was subtracted from the dispersion energy of the open pore form.

a)

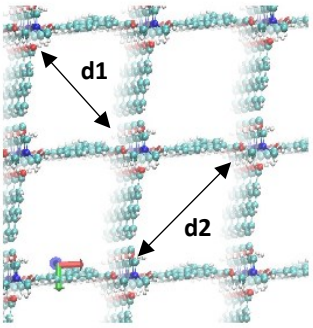

Initial *op* phase

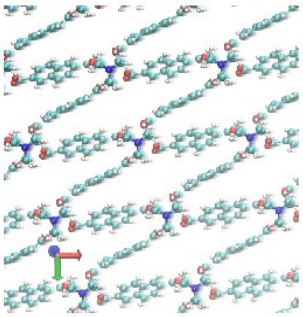

intermidiate phase after 1 ps

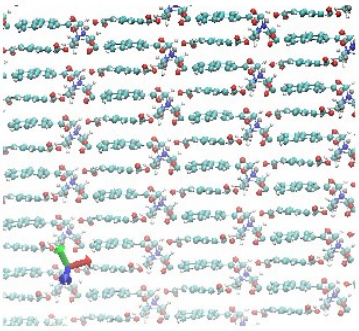

cp phase after 5.5 ps MD simulation

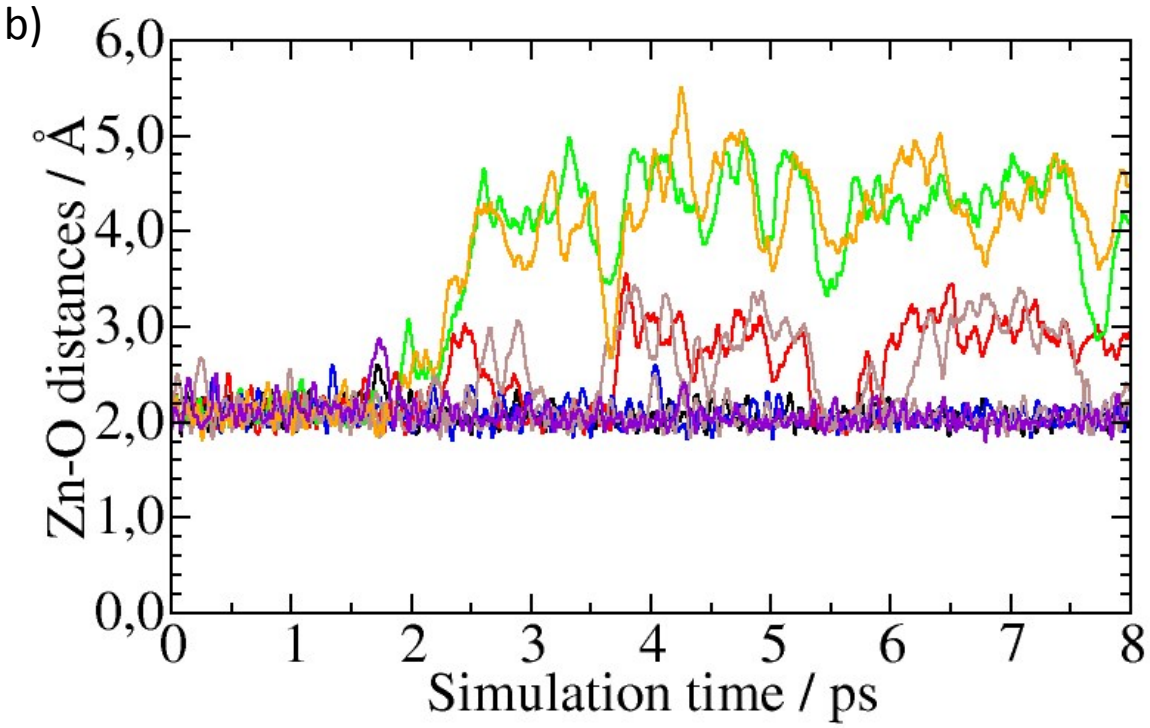

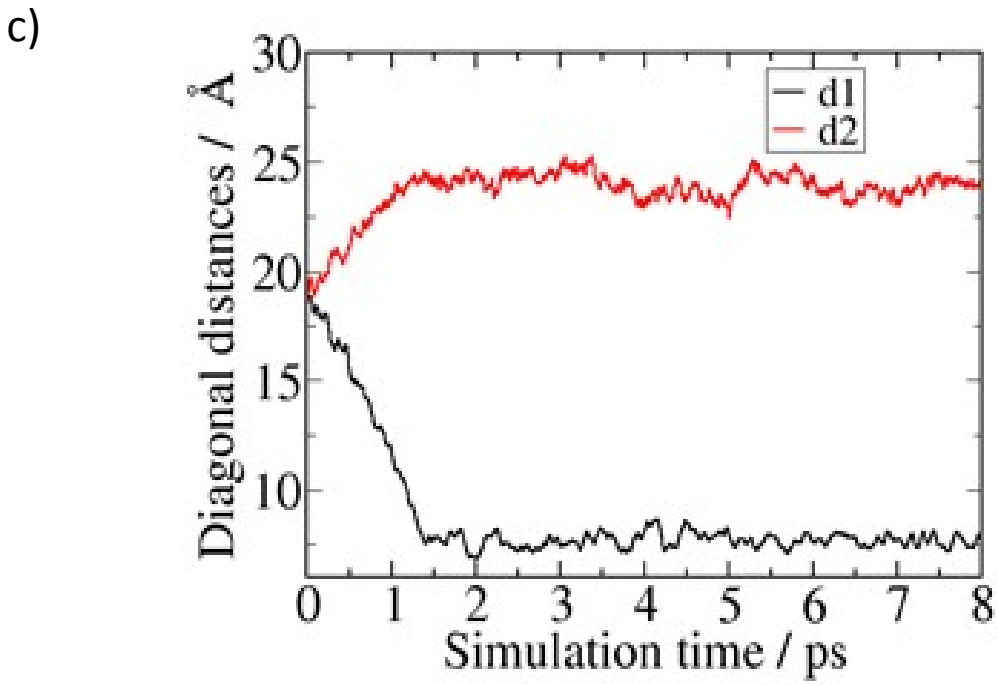

Figure S13. a) Snapshots from the *ab initio* MD (NPT) simulation at 300 K and 1 atm of DUT-8(Zn) starting from minimized *op* phase; b) changes in the Zn - O distances in the paddle wheel during the MD simulation, different colours represent each separate Zn - O distance in the paddle wheel; c) change in the diagonal distances of the square pore in the DUT-8(Zn) during the *op* - *cp* transformation in the MD simulation, when d1 = d2 the pore of the MOF is open , when d1 << d2 the pore is closed.

References

1. P. Maniam and N. Stock, *Inorg. Chem.*, 2011, **50**, 5085.
2. S. Ehrling, I. Senkovska, V. Bon, J. D. Evans, P. Petkov, Y. Krupskaya, V. Kataev, T. Wulf, A. Krylov, A. Vtyurin, S. Krylova, S. Adichtchev, E. Slyusareva, M. S. Weiss, B. Büchner, T. Heine and S. Kaskel, *J. Mater. Chem. A*, 2019, **7**, 21459.
3. H. Wang, J. Getzschmann, I. Senkovska and S. Kaskel, *Microporous Mesoporous Mater.*, 2008, **116**, 653.
4. D. N. Dybtsev, H. Chun and K. Kim, *Angew. Chem. Int. Ed.*, 2004, **43**, 5033.
5. P. S. Petkov, V. Bon, C. L. Hobday, A. B. Kuc, P. Melix, S. Kaskel, T. Düren and T. Heine, *Phys. Chem. Chem. Phys.*, 2019, **21**, 674.